

# Small- $x$ neutrino-hadron structure functions in charged current DIS within the QCD color dipole picture

M.B. GAY DUCATI<sup>a</sup>, M.M. MACHADO<sup>a</sup>, M.V.T. MACHADO<sup>b</sup>

<sup>a</sup> High Energy Physics Phenomenology Group, GFPAE, IF-UFRGS  
Caixa Postal 15051, CEP 91501-970, Porto Alegre, RS, Brazil

<sup>b</sup> Centro de Ciências Exatas e Tecnológicas, Universidade Federal do Pampa  
Campus de Bagé, Rua Carlos Barbosa. CEP 96400-970. Bagé, RS, Brazil

## Abstract

We present an exploratory QCD analysis of the neutrino structure functions in charged current DIS using the color dipole formalism. The corresponding dipole cross sections are taken from recent phenomenological/theoretical studies in deep inelastic inclusive production. The theoretical predictions are compared to the available experimental results in the small- $x$  region. In particular, the behavior of the structure functions on the boson virtuality and the role played by the nuclear shadowing corrections are investigated. It is demonstrated that small- $x$  neutrino-hadron cross section exhibits geometric scaling property as in lepton-hadron processes.

## 1 Introduction

The interaction of high energy neutrinos on hadron targets are an outstanding probe to test Quantum Chromodynamics (QCD) and understanding the parton properties of hadron structure. The several combinations of neutrino and anti-neutrino scattering data can be used to determine the structure functions, which constrain the valence, sea and gluon parton distributions in the nucleons/nuclei. The comparison between neutrino and charged-lepton experimental data can be also used to investigate the universality of the parton distributions. In particular, neutrino physics has received increasing interest due to the neutrino oscillations phenomenon in the context of solar and atmospheric neutrinos experiments. Moreover, the neutrino structure functions are needed for computing the total neutrino-hadron cross section, which plays an important role in high energy cosmic rays studies and in astroparticle physics [1].

The differential cross section for the neutrino-nucleon charged current process  $\nu_l (\bar{\nu}_l) + N \rightarrow l^- (l^+) + X$ , in terms of the Lorentz invariant structure functions  $F_2^{\nu N}$ ,  $2xF_1^{\nu N}$  and  $xF_3^{\nu N}$  are [2],

$$\frac{d\sigma^{\nu, \bar{\nu}}}{dx dy} = \frac{G_F^2 m_N E_\nu}{\pi} \left[ \left( 1 - y - \frac{m_N xy}{2E_\nu} \right) F_2(x, Q^2) + \frac{y^2}{2} 2xF_1(x, Q^2) \pm y \left( 1 - \frac{y}{2} \right) xF_3(x, Q^2) \right], \quad (1)$$

where  $G_F$  is the weak Fermi coupling constant,  $m_N$  is the nucleon mass,  $E_\nu$  is the incident neutrino energy,  $Q^2$  is the square of the four-momentum transfer to the nucleon. The variable  $y = E_{had}/E_\nu$  is the fractional energy transferred to the hadronic vertex with  $E_{had}$  being the measured hadronic energy, and  $x = Q^2/2m_N E_\nu y$  is the Bjorken scaling variable (fractional momentum carried by the struck quark).

Similarly to the charged-lepton DIS, the deep inelastic neutrino scattering is also used to investigate the structure of nucleons and nuclei. In the leading order quark-parton model (the QCD collinear approach), the structure function  $F_2$  is the singlet distribution,  $F_2^{\nu N} \propto xq^S = x \sum(q + \bar{q})$ , the sum of momentum densities of all interacting quarks constituents, and  $xF_3$  is the non-singlet distribution,  $xF_3^{\nu N} \propto xq^{NS} = x \sum(q - \bar{q}) = xu_V + xd_V$ , the valence quark momentum density. These relations are further modified by higher-order QCD corrections. For discussions of small- $x$  neutrino-hadron interaction within the perturbative (leading twist) QCD approach and its dependence on the parton pdf's, see Ref. [3]. Currently, the theoretical description of experimental data on neutrino DIS is reasonable (for a very recent investigation, see Ref. [4]). The main theory uncertainties are the role played by nuclear shadowing in contrast with lepton-charged DIS and a correct understanding of the low  $Q^2$  limit. The first uncertainty can be better addressed with the future precise data from MINER $\nu$ A [5] and neutrino-factory [6]. However, nuclear effects are taken into account by using the nuclear ratios  $R = F_2^A/AF_2^p$  extracted from lepton-nucleus DIS, which it could be different for the neutrino-nucleus case. The low- $Q^2$  region can not be addressed within the pQCD quark-parton model as a hard momentum scale  $Q_0^2 \geq 1 - 2 \text{ GeV}^2$  is required in order to perform perturbative expansion.

In this work we present a determination of the small- $x$  structure functions for neutrino-nucleus within the color dipole formalism [7]. This approach is also suitable for high energy neutrino interactions and naturally accounts for the correct low- $Q^2$  behavior of structure functions and address nuclear shadowing through the Glauber-Gribov formalism in the totally coherent limit [8]. The boson-hadron cross section is computed as the convolution of the distributions of color dipoles of definite transverse size created by splitting of the incident boson into a  $q\bar{q}$  pair. These distributions provide a clear relation between increasing  $Q^2$  and decreasing dipole size (or vice versa). The Glauber-Gribov theory considers the multiple scattering of the hadronic component of the virtual boson with a nucleus made of nucleons whose binding energy is neglected. This hadronic component keeps a fixed size during the scattering process (the eikonal approximation) and is usually limited to its lowest-order Fock state, the so-called dipole pair. The differences between realizations of this approach come from the model considered for the dipole-nucleon cross section. Several phenomenological implementations are able

to describe a wide range of inclusive/diffractive  $ep$  DIS data (see recent comparison in [9]) and experimental results for nuclear shadowing for  $x \leq 0.01$  [8]. In general, the transition to low- $Q^2$  limit is related to the saturation physics where an important quantity is the saturation scale,  $Q_{\text{sat}} \propto (E_\nu)^{\lambda/2}$ ,  $\lambda \simeq 0.3$ . This quantity sets the momentum scale where multiple scatterings become increasingly important. The color dipole approach allows an all twist computation in contrast with the usual leading twist approximation. One striking feature of the available saturation approaches is the prediction of the geometric scaling. Namely, the total photon-proton cross section at large energies is not a function of the two independent variables  $x$  and  $Q^2$ , but is rather a function of the single variable  $\tau_p = Q^2/Q_{\text{sat}}^2$ . As demonstrated in Ref. [11], the HERA data on the proton structure function  $F_2$  are consistent with scaling at  $x \leq 0.01$  and  $Q^2 \leq 400 \text{ GeV}^2$ . Similar behavior has been observed in exclusive [12], electron-nuclei processes [13], charm inclusive production [14] and diffractive DIS [15]. These results, while not entirely compelling, provide a strong motivation for investigations in the neutrino sector.

This paper is organized as follows. In Sec. 2, the neutrino structure function  $F_2^{\nu N}$  is investigated within the color dipole picture at small- $x$  region. We employ recent phenomenological parton saturation models, which are successful in describing inclusive deep inelastic data. Nuclear effects are taken into account through Glauber-Gribov formalism and the results are compared to accelerator data. It is demonstrated that the small- $x$  neutrino-hadron data exhibit geometric scaling property, which has important consequences for ultra-high energy neutrino phenomenology. In Sec. 3, the structure functions  $x F_3$  and  $2x F_1$  are addressed, pointing out their left-right asymmetry and consequences to the effects of nuclear shadowing. In addition, the quantity  $\Delta x F_3 = x F_3^\nu - x F_3^{\bar{\nu}}$  is investigated, which provides a determination of the strange-sea parton distribution through charm production in charged-current neutrino DIS. Finally, in the last section we present comments and conclusions.

## 2 Neutrino Structure Function $F_2^{\nu N}(x, Q^2)$

Deep inelastic neutrino scattering can proceed via  $W^\pm$  or  $Z^0$  exchanges. The first case corresponds to charged current (CC) and the second one to the neutral current (NC) interactions. The standard kinematical variables which describe the processes above are given by,  $s = 2 m_N E_\nu$ ,  $Q^2 = -q^2$  and  $x = \frac{Q^2}{2p \cdot q}$ . Here,  $m_N$  is the nucleon mass,  $E_\nu$  labels the neutrino energy and  $p$  and  $q$  are the four momenta of the nucleon and of the exchanged boson, respectively. One assumes an isoscalar target  $N = (p + n)/2$ , which is a good approximation for the present purpose.

We focus here in the high energy regime, which one translates into small- $x$  kinematical region. At this domain a quite successful framework to describe QCD interactions is provided by the color dipole formalism [7], which allows an all twist computation (in contrast with the usual leading twist approximation) of the structure functions. The physical picture of the

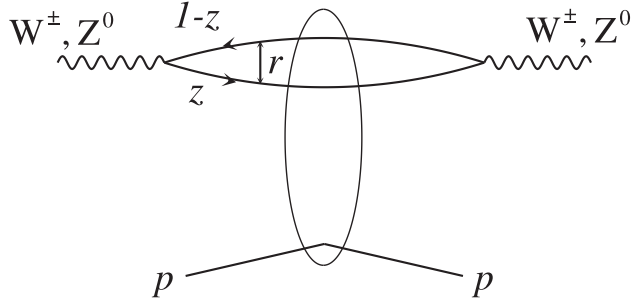


Figure 1: Boson-hadron scattering in the color dipole picture (figure from [18]).

interaction is the deep inelastic scattering at low  $x$  viewed as the result of the interaction of a color  $q\bar{q}$  color dipole, in which the gauge boson fluctuates into, with the nucleon target. The interaction is modeled via the dipole-target cross section, whereas the boson fluctuation in a color dipole is given by the corresponding wave function (see Fig. 1). The CC DIS structure functions for neutrino-nucleon scattering in the dipole picture [16, 17, 18] are related to the cross section for scattering of transversely and longitudinally polarized  $W^\pm$  bosons. That is,

$$F_{T,L}^{\text{CC}}(x, Q^2) = \frac{Q^2}{4\pi^2} \int d^2\mathbf{r} \int_0^1 dz |\psi_{T,L}^{W^\pm}(z, \mathbf{r}, Q^2)|^2 \sigma_{dip}(x, \mathbf{r}), \quad (2)$$

where  $\mathbf{r}$  denotes the transverse size of the color dipole,  $z$  the longitudinal momentum fraction carried by a quark and  $\psi_{T,L}^{W^\pm}$  are the light-cone wavefunctions for (virtual) charged gauge bosons with transverse or longitudinal polarizations. The small- $x$  neutrino structure function  $F_2^{\nu N}$  is computed from expressions above taking  $F_2 = F_T + F_L$ . Explicit expressions for the wave functions squared are given by [16, 17, 18],

$$|\psi_T^{W^\pm}|^2 = \frac{4N_c}{(2\pi)^2} \left\{ [(1-z)^2 m_q + z^2 m_{\bar{q}}^2] K_0^2(\varepsilon r) + [z^2 + (1-z)^2] \varepsilon^2 K_1^2(\varepsilon r) \right\}, \quad (3)$$

$$|\psi_L^{W^\pm}|^2 = \frac{4N_c}{(2\pi)^2 Q^2} \left\{ [(z(1-z)Q^2 + \varepsilon^2)^2 + m_q^2 m_{\bar{q}}^2] K_0^2(\varepsilon r) + \left[ \frac{a_-^2 + a_+^2}{2} \right] \varepsilon^2 K_1^2(\varepsilon r) \right\}, \quad (4)$$

where one defines the auxiliary variable  $\varepsilon^2 = z(1-z)Q^2 + (1-z)m_q^2 + zm_{\bar{q}}^2$ ,  $K_{0,1}(u)$  are the McDonald's functions and  $a_+ = (m_q + m_{\bar{q}})$ ,  $a_- = (m_q - m_{\bar{q}})$ . The quark and anti-quark masses are named by  $m_q$  and  $m_{\bar{q}}$ , respectively. The expressions above reduce to the well known case for equal flavor quarks,  $m_q = m_{\bar{q}} = m_f$ . In what follows we consider four quark flavors ( $u, d, s, c$ ) with masses  $m_f$ . It has been shown [19] that heavy quarks ( $b, t$ ) give relatively small contribution for total neutrino cross section and it is not important for the kinematical range considered in this study. Moreover, the color dipoles contributing to Cabibbo favored transitions are  $u\bar{d}$  ( $d\bar{u}$ ),  $c\bar{s}$  ( $s\bar{c}$ ) for CC interactions. A generalization for NC interactions is also known [18].

The dipole hadron cross section  $\sigma_{dip}$  contains all information about the target and the strong interaction physics. There are several phenomenological implementations for this quantity and the main feature is to be able to match the soft (low  $Q^2$ ) and hard (large  $Q^2$ ) regimes in an unified way. In the present study, we consider analytical expressions for the dipole cross section, with particular interest for those ones presenting scaling behavior. Namely, one has  $\sigma_{dip} \propto (\mathbf{r}^2 Q_{\text{sat}}^2)^\gamma$  for dipole sizes  $\mathbf{r}^2 \approx 1/Q_{\text{sat}}^2$  and where  $\gamma$  is the effective anomalous dimension. The so-called saturation scale  $Q_{\text{sat}} \propto x^{\lambda/2}$  defines the onset of the parton saturation effects. In what follows one takes the phenomenological parameterizations: (a) Golec-Biernat-Wüsthoff model (GBW) [20] and (b) Itakura-Iancu-Munier (IIM) model [21]. Both models are able to describe experimental data on inclusive and diffractive deep inelastic  $ep$  scattering at small- $x$ . Let us summarize the main features of each model. The GBW parameterization takes the eikonal-like form,

$$\sigma_{dip}(x, \mathbf{r}^2) = \sigma_0 \left[ 1 - \exp\left(-\frac{\mathbf{r}^2 Q_{\text{sat}}^2}{4}\right) \right], \quad Q_{\text{sat}}^2(x) = \left(\frac{x_0}{\bar{x}}\right)^\lambda \text{ GeV}^2. \quad (5)$$

where the parameters were obtained from a fit to the HERA data [20]. An additional parameter is the effective light quark mass,  $m_f = 0.14$  GeV, which plays the role of a regulator at the photoproduction limit [20]. Here,  $\bar{x} = x[1 + (4m_f^2/Q^2)]$ . The charm mass is set to be  $m_c = 1.5$  GeV. The GBW model presents a geometric scaling form,  $\sigma_{dip} \propto f(\mathbf{r}^2 Q_{\text{sat}}^2)$ . For small dipoles  $\mathbf{r}^2 \leq 1/Q_{\text{sat}}^2$  it can be approximated by  $\sigma_{dip} \simeq \sigma_0(\mathbf{r}^2 Q_{\text{sat}}^2/4)$ , where the effective anomalous dimension is equal one,  $\gamma = 1$ .

Although the GBW model has being very successful in describing HERA data, its functional form is only an approximation of the theoretical non-linear QCD approaches. An analytical expression for the dipole cross section can be obtained within the BFKL formalism and intense theoretical studies have been performed towards an understanding of the BFKL approach in the border of the saturation region, e.g. [12]. In particular, the dipole cross section was calculated in both LO and NLO BFKL approaches in the geometric scaling region [22]. The IIM parameterization smoothly interpolates between the limiting behaviors analytically under control: the solution of the BFKL equation for small dipole sizes,  $\mathbf{r} \ll 1/Q_{\text{sat}}(x)$ , and the Levin-Tuchin prediction [23] for larger ones,  $\mathbf{r} \gg 1/Q_{\text{sat}}(x)$ . A fit to the structure function  $F_2(x, Q^2)$  was performed in the kinematical range of interest. The IIM dipole cross section is parameterized as follows,

$$\sigma_{dip}^{\text{IIM}}(x, \mathbf{r}) = \sigma_0 \begin{cases} \mathcal{N}_0 \left(\frac{\bar{\tau}^2}{4}\right)^{\gamma_{\text{eff}}(x, r)}, & \text{for } \bar{\tau} \leq 2, \\ 1 - \exp[-a \ln^2(b\bar{\tau})], & \text{for } \bar{\tau} > 2, \end{cases}$$

where  $\bar{\tau} = \mathbf{r}Q_{\text{sat}}(x)$  and the expression for  $\mathbf{r}Q_{\text{sat}}(x) > 2$  (saturation region) is an adequate functional form, compatible with approximate or asymptotic solutions of the Balitsky-Kovchegov (BK) [24] equation and Color Glass Condensate (CGC) formalism [25]. The coefficients  $a$  and  $b$  are determined from the continuity conditions of the dipole cross section at  $\mathbf{r}Q_{\text{sat}} = 2$ . The coefficients  $\gamma_{\text{sat}} = 0.63$  (the BFKL anomalous dimension at the saturation border) and  $\kappa = 9.9$

are fixed from their LO BFKL values. The IIM parameterization presents scaling violation once the effective anomalous dimension depends also on the rapidity  $Y = \ln(1/x)$  for small size dipoles,  $\gamma(x, \mathbf{r}) = \gamma_{\text{sat}} + \frac{\ln(2/\mathbf{r}Q_{\text{sat}})}{\kappa \lambda Y}$ . For small dipoles having transverse size relatively close to  $R_{\text{sat}}$  the second term vanishes and the dipole cross section scales as  $\sigma_{dip} \propto \sigma_0 (\mathbf{r}^2 Q_{\text{sat}}^2/4)^{\gamma_{\text{sat}}}$ .

Some remarks are in order here. The color dipole models are suitable in the region below  $x = 0.01$  and the large  $x$  limit still needs a consistent treatment. Making use of the dimensional-cutting rules (see Ref. [26] for a recent discussion), we supplement the dipole cross sections with a threshold factor  $(1-x)^{n_{\text{thres}}}$ , taking  $n_{\text{thres}} = 5$  for a 3-flavor analysis and  $n_{\text{thres}} = 7$  for a 4-flavor one. Moreover, for the extension of the approach to consider nuclei targets we take the Glauber-Gribov picture [8], without any new parameter. In this approach, the nuclear version is obtained replacing the dipole-nucleon cross section by the nuclear one,

$$\sigma_{dip}^{\text{nucleus}}(\tilde{x}, \mathbf{r}^2; A) = 2 \int d^2b \left\{ 1 - \exp \left[ -\frac{1}{2} T_A(b) \sigma_{dip}^{\text{nucleon}}(\tilde{x}, \mathbf{r}^2) \right] \right\}, \quad (6)$$

where  $b$  is the impact parameter of the center of the dipole relative to the center of the nucleus and the integrand gives the total dipole-nucleus cross section for a fixed impact parameter. The nuclear profile function is labeled by  $T_A(b)$ , which will be obtained from a 3-parameter Fermi distribution for the nuclear density [27]. The above equation sums up all the multiple elastic rescattering diagrams of the  $q\bar{q}$  pair and is justified for large coherence length, where the transverse separation  $\mathbf{r}$  of partons in the multiparton Fock state of the photon becomes as good a conserved quantity as the angular momentum, *i. e.* the size of the pair  $\mathbf{r}$  becomes eigenvalue of the scattering matrix. Therefore, the region of applicability of these models should be at small values of  $x$ , *i. e.* large coherence length, and for not too high values of virtualities. In our further investigation of the neutrino structure functions we concentrate on that kinematical region.

A basic property of the saturation physics is the the geometric scaling. When applied to the deep inelastic scattering it means that the total  $\gamma^*p$  cross section at large energies is not a function of the two independent variables  $x$  and  $Q$ , but is rather a function of the single variable  $\tau_p = Q^2/Q_{\text{sat}}^2(x)$  as shown in Ref. [11]. Recently, the high energy lepton-hadron, proton-nucleus and nucleus-nucleus collisions have been related through geometric scaling [28]. Within the color dipole picture and making use of a rescaling of the impact parameter of the  $\gamma^*h$  cross section in terms of hadronic target radius  $R_h$ , the nuclear dependence of the  $\gamma^*A$  cross section is absorbed in the  $A$ -dependence of the saturation scale via geometric scaling. The relation reads as

$$\sigma_{tot}^{\gamma^*A}(\tau_A) = \frac{\pi R_A^2 \sigma_{tot}^{\gamma^*p}(\tau_A)}{\pi R_p^2}, \quad \tau_A = \tau_p \left( \frac{\pi R_A^2}{A\pi R_p^2} \right)^\Delta, \quad (7)$$

where the nuclear saturation scale was assumed to rise with the quotient of the transverse parton densities to the power  $\Delta = 1/\delta$  and  $R_A$  is the nuclear radius. The nucleon saturation momentum is taken from GBW model[20]. The following functional shape (scaling curve) for

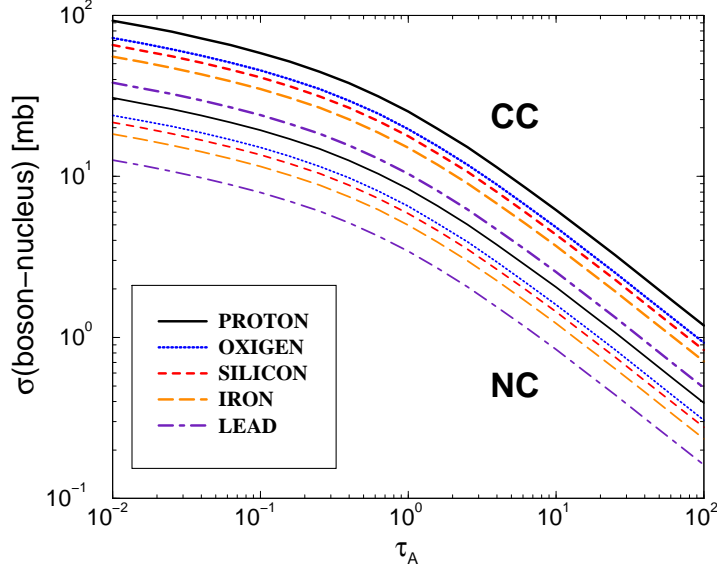


Figure 2: Geometric scaling for the electroweak boson-nucleus cross section as a function of the scaling variable  $\tau_A$  for different atomic numbers (normalized to nucleon).

the photoabsorption cross section has been considered based on theoretical studies, e.g. Glauber-Mueller approach [28]:

$$\sigma_{tot}^{\gamma^*p}(\tau_p) = \bar{\sigma}_0 [\gamma_E + \Gamma(0, \beta) + \ln(\beta)], \quad \beta = a/\tau_p^b, \quad (8)$$

where  $\gamma_E$  is the Euler constant and  $\Gamma(0, \beta)$  the incomplete Gamma function. The parameters for the proton (nucleon) case were obtained from a fit to the small- $x$   $ep$  DESY-HERA data, with the overall normalization fixed by  $\bar{\sigma}_0 = 40.56 \mu b$ . The parameters for the nuclear saturation scale were determined by fitting the available lepton-hadron data using the relation in Eq. (7) and the same scaling function, Eq. (8).

The theoretical and phenomenological achievements summarized above have direct consequences on the computation of small- $x$  neutrino structure functions. A very important feature is that, within the color dipole framework [7], the charged and neutral current structure functions are described by the same mathematical expressions as the proton structure function up to a different coupling of the electroweak bosons. Therefore, the geometric scaling property should be present also in neutrino scattering on hadron targets and allows to obtain the dependences on energy and atomic number of CC/NC cross sections, which are encoded in the nuclear saturation momentum. In what follows, the weak boson-hadron/nucleus cross section is computed and it is shown to exhibit geometric scaling on the scaling variable  $\tau_A$ . This fact has been investigated in detail at Refs. [29, 30]. Based on the fact that the expressions for the photon wavefunction and the electroweak gauge bosons are exactly the same up to the different coupling of the bosons to the quark color dipole, we can simply write,

$$\sigma_{tot}^{(W^\pm N)}(x, Q^2; A) = \frac{4}{\alpha_{em} \sum_f e_f^2} \sigma_{tot}^{(\gamma^* N)}(x, Q^2; A), \quad (9)$$

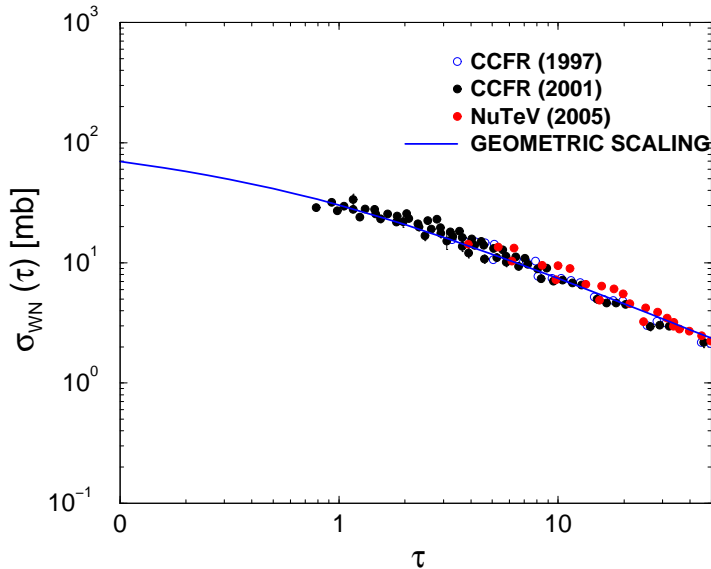


Figure 3: The scaling behavior of  $\sigma_{WN}(x, Q^2)$  from experimental data for  $F_2^{\nu N}$  as a function of scaling variable  $\tau$  (see text).

where  $\alpha_{\text{em}}$  is the QED constant coupling,  $e_f$  is the electric charge of the quark of flavor  $f$ . The scaling present in the lepton-hadron cross section at high energies, as quantified by Eq. (7) and further experimentally demonstrated, is automatically translated to the UHE neutrino scattering on nucleon or nucleus. For illustration, in Fig. 2 one presents the boson-hadron cross sections, Eq. (9), as a function of the scaling variable  $\tau_A$  for distinct nucleus as well as for the nucleon. They are normalized to the nucleon. The cross sections exhibit geometric scaling, verifying a transition in the behavior on  $\tau_A$  of the cross section from a smooth dependence at small  $\tau_A$  and an approximated  $1/\tau$  behavior at large  $\tau_A$ . Similarly to the lepton-hadron case, the transition point is placed at  $\tau_A = 1$ . The asymptotic  $1/\tau^b$  dependence reflects the fact that the cross section scales as  $Q_{\text{sat}}^2/Q^2$  modulo logarithmic corrections, with energy dependence driven by the saturation scale. The mild dependence at  $\tau_A \leq 1$  corresponds to the fact that the cross section scales as  $\propto \sigma_0 \log(Q_{\text{sat}}^2/m_f^2)$  towards  $Q^2 \rightarrow 0$  limit.

It is important to investigate whether this geometric scaling pattern is exhibited by the small- $x$  neutrino deep inelastic data. In order to do so, we take the datasets for the structure function  $F_2$  with the kinematical cut  $x \leq 0.035$  and all  $Q^2$  [31, 32, 33]. We plot the quantity  $\sigma_{W^{\pm N}} = \frac{4\pi^2}{Q^2} F_2$  as a function of the scaling variable  $\tau_p = Q^2/Q_{\text{sat}}^2(x)$ . The saturation scale squared reads as  $Q_{\text{sat}}^2(x) = (3 \cdot 10^{-4}/x)^{0.288}$  [20]. The geometric scaling behavior is present with a smooth spread around the scaling curve. The scaling curve (solid line) is obtained using Eq. (9) and the functional shape in Eq. (8). This result is useful and can be investigated in more detail using precise measurements in future experiments. In the present kinematical window, the color dipole formalism (and geometric scaling property) is in the limit of its validity. However, the present result shows that it gives a reasonable phenomenological description of

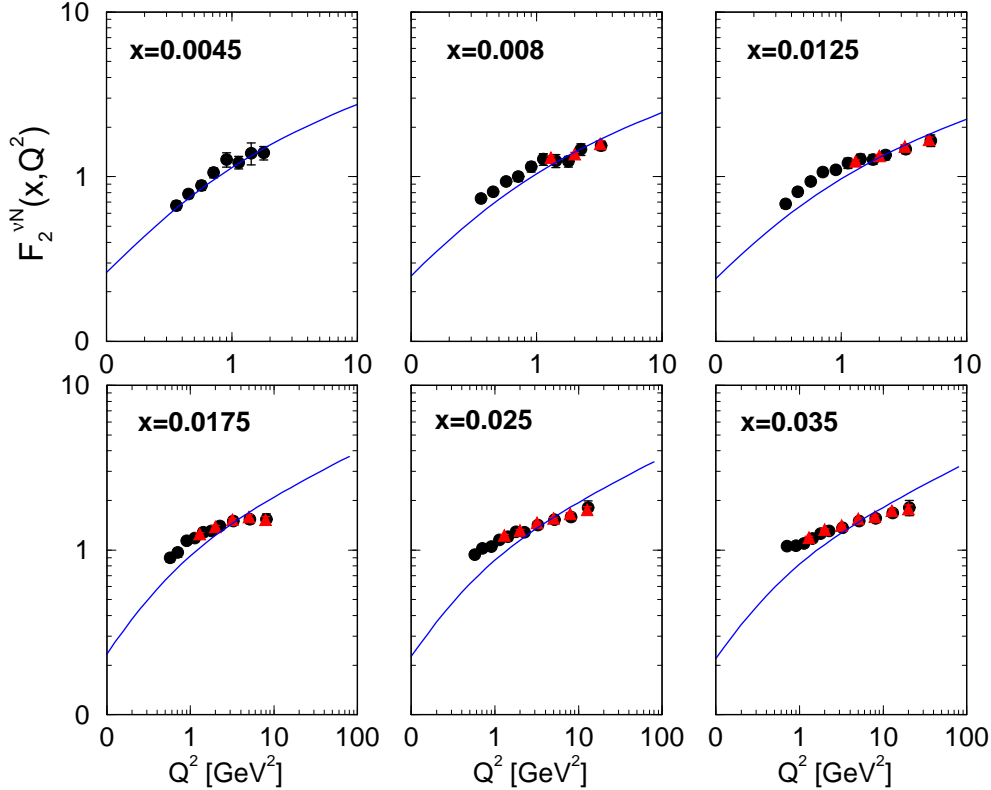


Figure 4: The structure function  $F_2^{\nu N}(x, Q^2)$  as a function of boson virtuality. Theoretical curve corresponds the geometric scaling result for the neutrino-nucleus interactions (see text). Experimental data from CCFR Collaboration [31, 32].

the limit case.

Finally, we will compare the color dipole prediction against the  $F_2^{\nu N}$  structure function. We use the experimental datasets of the CCFR Collaboration [31, 32], where filled circles correspond to points in Ref. [32] and triangles up correspond to points in Ref. [31]. The solid curve is obtained using scaling property and nuclear shadowing from Glauber-Gribov formalism is also included (estimated to be of order 20% at small- $x$ ). The data description is reasonable up to  $x \simeq 0.0175$ , just in the border of the expected validity region of the color dipole approach. For completeness, we show the larger  $x$  data points. The valence content has not been included and it could improve the description in that region. It is worth to mention the robustness of the color dipole formalism as the theoretical curves were obtained without any tuning of the original model parameters obtained in  $ep$  HERA data.

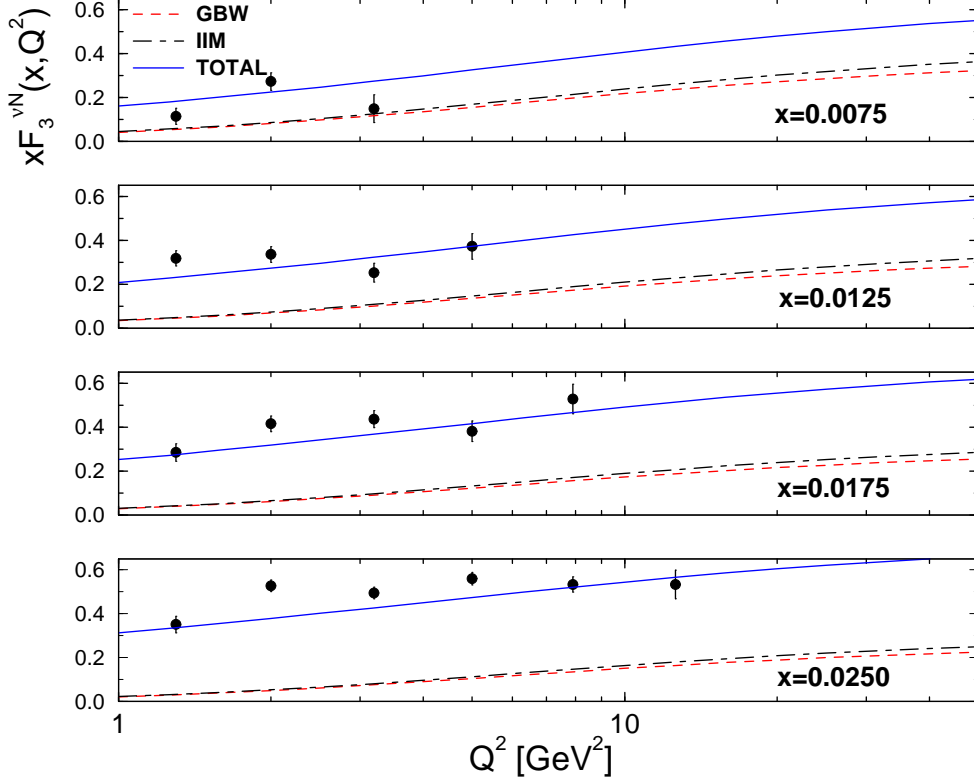


Figure 5: The structure function  $x F_3^{\nu N}(x, Q^2)$  as a function of boson virtuality. Theoretical curves correspond to the results using the GBW (dashed) and the IIM (dot-dashed) models for dipole cross section, respectively. The total contribution (solid) includes the valence quark contribution. Experimental data from CCFR Collaboration [31].

### 3 The functions $x F_3^{\nu N}$ , $2x F_1^{\nu N}$ and the quantity $\Delta x F_3^{\nu N}$

Lets now compute the structure functions  $x F_3^{\nu N}$  and  $2x F_1^{\nu N}$  within the color dipole formalism. We concentrate on the the interaction of the  $c\bar{s}$  color dipole of size  $\mathbf{r}$  with the target hadron which is described by the beam- and flavor-independent color dipole cross section  $\sigma_{dip}$ . In the infinitum momentum frame, this is equivalent to the  $W^\pm$ -gluon fusion process,  $W^\pm + g \rightarrow c\bar{s}(\bar{c}s)$ . The analysis for charged current DIS has been addressed in Refs. [34, 35], where the left-right asymmetry of diffractive interactions of electroweak bosons of different helicity is discussed. There, the relevant light-cone wavefunctions have been evaluated. The contribution of excitation of open charm/strangeness to the hadron absorption cross section for left-handed ( $L$ ) and right-handed ( $R$ )  $W$ -boson of virtuality  $Q^2$ , is given by [7],

$$\sigma_{L,R}(x, Q^2) = \int d^2\mathbf{r} \int_0^1 dz \sum_{\lambda_1, \lambda_2} |\Psi_{L,R}^{\lambda_1, \lambda_2}(z, \mathbf{r}, Q^2)|^2 \sigma_{dip}(x, \mathbf{r}), \quad (10)$$

where  $\Psi_{L,R}^{\lambda_1,\lambda_2}(z, \mathbf{r}, Q^2)$  is the light-cone wavefunction of the  $c\bar{s}$  state with the  $c$  quark carrying fraction  $z$  of the  $W^+$  light-cone momentum and  $\bar{s}$  with momentum fraction  $1 - z$ . The  $c$ - and  $\bar{s}$ -quark helicities are  $\lambda_1 = \pm 1/2$  and  $\lambda_2 = \pm 1/2$ , respectively. The diagonal elements of density matrix are given by,

$$\sum_{\lambda_1,\lambda_2} \Psi_L^{\lambda_1,\lambda_2} \left( \Psi_L^{\lambda_1,\lambda_2} \right)^* = \frac{4 N_c}{(2\pi)^2} z^2 \left[ m_{\bar{q}}^2 K_0^2(\varepsilon r) + \varepsilon^2 K_1^2(\varepsilon r) \right], \quad (11)$$

$$\sum_{\lambda_1,\lambda_2} \Psi_R^{\lambda_1,\lambda_2} \left( \Psi_R^{\lambda_1,\lambda_2} \right)^* = \frac{4 N_c}{(2\pi)^2} (1 - z)^2 \left[ m_q^2 K_0^2(\varepsilon r) + \varepsilon^2 K_1^2(\varepsilon r) \right]. \quad (12)$$

In the expressions given by Eqs. (11)-(12), one uses the notation  $\varepsilon^2 = z(1-z)Q^2 + (1-z)m_q^2 + zm_{\bar{q}}^2$ , where the quark and antiquark masses are  $m_q$  and  $m_{\bar{q}}$ , respectively. The corresponding expressions for  $W^-$  boson are obtained by replacing  $m_q \leftrightarrow m_{\bar{q}}$ . It should be noticed the strong left-right asymmetry referred above.

The structure function of deep inelastic neutrino-nucleon  $x F_3$  can be defined in terms of  $\sigma_R$  and  $\sigma_L$  of Eq. (10) in the following usual way,

$$x F_3^{\nu N}(x, Q^2) = \frac{Q^2}{4\pi^2} \left[ \sigma_L(x, Q^2) - \sigma_R(x, Q^2) \right]. \quad (13)$$

where the expression can be interpreted in terms of parton densities as being the sea-quark component of  $x F_3$ . It corresponds to the excitation of the  $c\bar{s}$  state in the process  $W^+ g \rightarrow c\bar{s}$ , with  $x F_3$  differing from zero due to the strong left-right asymmetry of the light-cone  $|c\bar{s}\rangle$  Fock state. For values of Bjorken variable not so small,  $x F_3$  contains important valence quark contribution. The valence term,  $x q_{val}$ , is the same for both  $\nu N$  and  $\bar{\nu} N$  structure functions of an iso-scalar nucleon. The sea-quark ( $x q_{sea}$ ) term in the  $x F_3^{\nu N}$  has opposite sign for  $x F_3^{\bar{\nu} N}$ , leading to  $x F_3^{\nu(\bar{\nu})N} = x q_{val} \pm x q_{sea}$ .

A direct comparison of result in Eq. (13) with experimental data is somewhat difficult. The reason is that structure functions obtained from neutrino scattering experiments are usually extracted from the sum and the difference of the neutrino and anti-neutrino  $y$ -dependent differential cross sections, respectively. That is,  $x F_3$  is determined by the average  $\frac{1}{2}(x F_3^{\nu N} + x F_3^{\bar{\nu} N})$ . In Ref. [34], the authors intend to compare the result of Eq. (13) to CCFR data [31]. However, this procedure is questionable since the  $c\bar{s}$  ( $s\bar{c}$ ) component disappears in the sum  $F_3^\nu + F_3^{\bar{\nu}} = 2x q_{val}$ . In order to make a rough comparison to give a phenomenological motivation, we use the following procedure. Considering that the sea content is approximately one half of the valence (see next analysis) in the kinematical range considered here, we rescale the experimental data by a factor  $3/2$ . This is a rough estimation of the nucleon structure function  $x F_3^{\nu N}$ . This comparison is shown in Fig. 5, where the structure function  $x F_3^{\nu N}(x, Q^2)$  is shown as a function of  $Q^2$ . The theoretical curves correspond to the results using the GBW (dashed-line) and the IIM (dot-dashed line) models for dipole cross section, respectively. The total contribution (solid) includes the valence quark contribution through the above procedure. The calculation takes

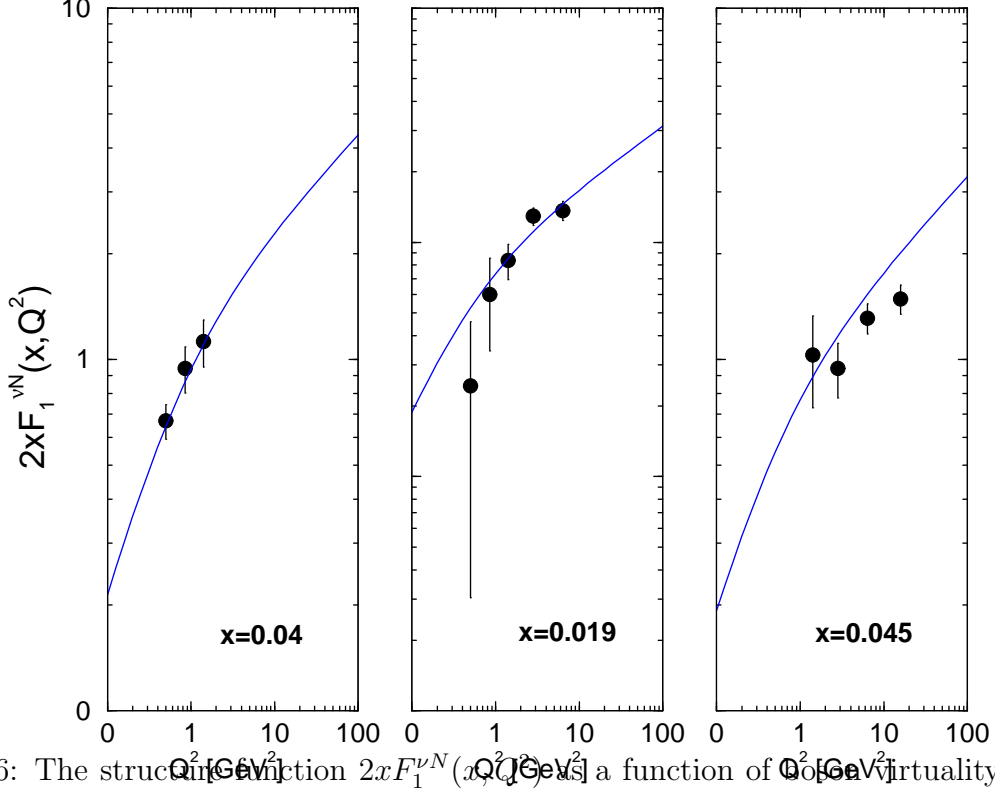


Figure 6: The structure function  $2xF_1^{vN}(x, Q^2)$  as a function of  $Q^2$  [GeV<sup>2</sup>] virtuality. Theoretical curve corresponds to the results using IIM model for dipole cross section. Experimental results from CCFR Collaboration [37].

into account nuclear shadowing for the iron nucleus via Glauber-Gribov formalism, where the dipole-nucleus cross section is computed using Eq. (6). In order to be consistent with the parameters of the models, we take  $m_f = 0.14$  GeV for light quarks and  $m_c = 1.5$  GeV for charm quark. The experimental data are from CCFR Collaboration [31]. The phenomenological results are in good agreement with the experimental measurements. The distinct models for the dipole cross section give similar results for the range of virtuality considered in the plots. We have checked our results with those in Ref. [34] and it was found they are similar despite the different dipole cross section used.

The structure function  $2xF_1$  can be also computed within the color dipole approach. It is proportional to the transverse contribution for the boson-hadron cross section. The complete expression reads as,

$$2xF_1(x, Q^2) = \frac{Q^2}{4\pi^2} [\sigma_L(x, Q^2) + \sigma_R(x, Q^2)] , \quad (14)$$

where now one takes the quark-antiquark pairs contributing to Cabibbo favored transitions.

We present the theoretical results in comparison with the CCFR Collaboration measurements [37] of the structure function  $2xF_1$  as a function of  $Q^2$  for three fixed values of  $x$  are shown in Fig. 6. There is good agreement between theory and data.

The neutrino-antineutrino difference  $xF_3^\nu - xF_3^{\bar{\nu}}$  provides a determination of the sea (strange) density. In the parton model, one has  $xF_3^{\nu N} = xq_{val} - 2x\bar{c}(x) + 2xs(x)$  and  $xF_3^{\bar{\nu}N} = xq_{val} + 2xc(x) - 2x\bar{s}(x)$ . Therefore, the neutrino-antineutrino difference effectively measures the strange density, since the charm contribution is small in the kinematical region measured by current experiments. Assuming  $s(x) = \bar{s}(x)$  and  $c(x) = \bar{c}(x)$  one obtains,

$$\Delta xF_3 = xF_3^{\nu N} - xF_3^{\bar{\nu}N} = 2xq_{sea} = 4x[s(x) - c(x)]. \quad (15)$$

Here, some comments are in order. Taking into account that our calculation in Eq. (13) corresponds to sea-quark content of  $xF_3$ , then  $\Delta xF_3 = 2xF_3^{\nu N}$ . Our calculation is equivalent to the  $cs$  component of the structure function given by the  $W$ -gluon fusion term at order  $\alpha_s$ , which reads as,

$$F_3^{\nu N}(W^+g \rightarrow c\bar{s}) = \left(\frac{\alpha_s}{2\pi}\right) \int_{ax}^1 \frac{dz}{z} g(z, \mu^2) C_3\left(\frac{x}{z}, Q^2\right), \quad (16)$$

where  $a = 1 + (m_c^2 + m_s^2)/Q^2$  and the Wilson coefficient  $C_3$  represents the  $W^+g \rightarrow c\bar{s}$  cross section. The total  $cs$  contribution to  $F_3$  is the sum of the quark excitation term, taken at the factorization scale  $\mu^2 = m_c^2$  (near threshold), and the gluon-fusion term above. Namely,

$$F_3^{\nu N}(x, Q^2) = 2[\bar{s}(x_c, \mu^2) - c(x, \mu^2)] + F_3^{\nu N}(W^+g \rightarrow c\bar{s}), \quad (17)$$

with the slow-rescaling variable  $x_c = x[1 + (m_c/Q^2)]$  and similar expression for  $F_3^{\bar{\nu}N}(x, Q^2)$ .

In Fig. 6 the quantity  $\Delta xF_3$  as a function of  $Q^2$  at fixed  $x$  is shown in comparison with the CCFR result obtained from  $\nu_\mu Fe$  and  $\bar{\nu}_\mu Fe$  differential cross section [36]. The theoretical curve is obtained from Eq. (15) using the IIM dipole cross section and Glauber-Gribov shadowing corrections. The agreement is good and the quark excitation contribution, described in Eq. (17), has not been added. This additional piece should improve the description.

## 4 Comments and Conclusions

As a summary, an analysis of small- $x$  neutrino-nucleus DIS is performed within the color dipole formalism. The structure functions  $F_2^{\nu N}$ ,  $xF_3^{\nu N}$ ,  $2xF_1^{\nu N}$  and the quantity  $\Delta xF_3^{\nu N}$  are calculated and compared with the experimental data from CCFR and NuTeV by employing phenomenological parameterizations for the dipole cross section which successfully describe small- $x$  inclusive and diffractive  $ep$  DIS data. Nuclear shadowing is taken into account through Glauber-Gribov formalism. It is found that small- $x$  data show geometric scaling property for the boson-hadron cross section as a function of the scaling variable  $\tau_p$ . The structure function  $F_2$  is in agreement with the phenomenological implementation using the saturation models at the region  $x \leq 0.0175$ . This is in agreement with the regime of validity of the color dipole approach. The structure functions  $xF_3^{\nu N}$  and  $2xF_1^{\nu N}$  are also in agreement with the experimental data.

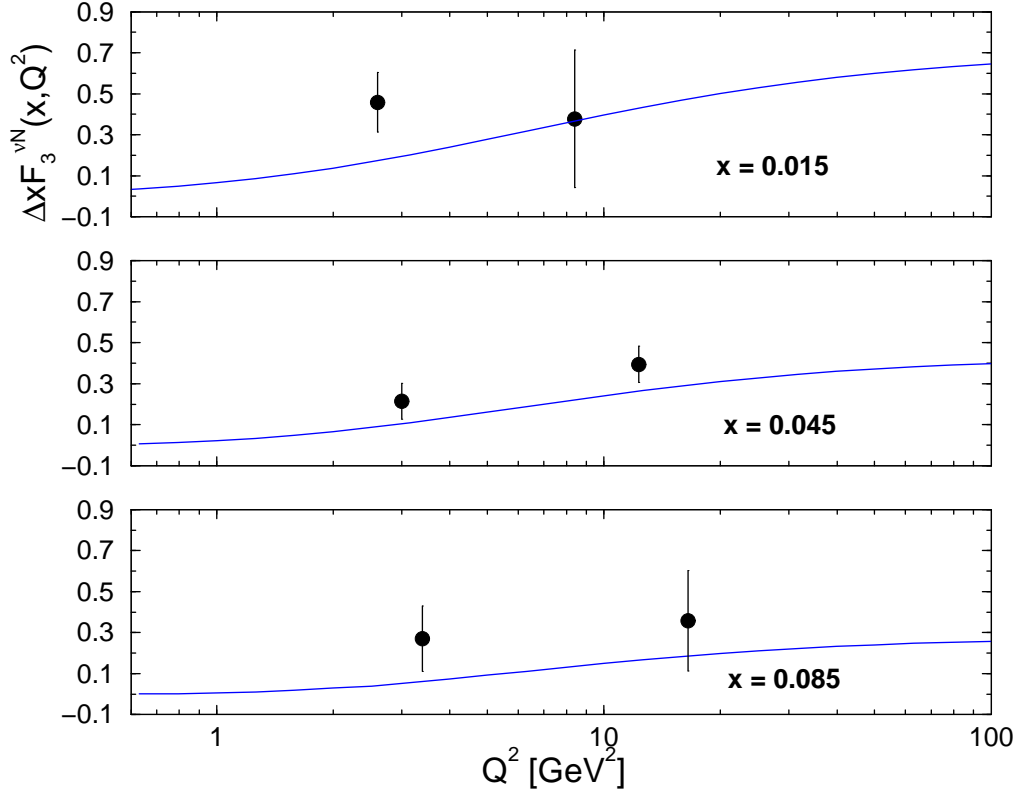


Figure 7: The structure function  $\Delta xF_3^{\nu N} = xF_3^{\nu N}(x, Q^2) - xF_3^{\bar{\nu} N}(x, Q^2)$  as a function of boson virtuality. Theoretical curve corresponds to the results using IIM model for dipole cross section. Experimental data from CCFR Collaboration.

The sea content, described by the quantity  $\Delta xF_3^{\nu N}$ , is well described and the addition of quark excitation term should improve it. Although the results presented here are compelling, further investigations are requested. In particular, measurements of neutrino-nucleus structure function in smaller values of  $x$  than the currently measured in the accelerator experiments. The present results also confirms the safe use of color dipole formalism to describe the total neutrino cross section of ultrahigh energy neutrinos as it is dominated by small- $x$  contributions.

## Acknowledgements

We thank Donna Naples and U. K. Yang for providing us with the experimental datasets of CCFR Coll. measurements on neutrino-nucleus structure functions. This work is supported by CNPq (Brazil).

## References

- [1] A.M. Staśto, *Int. J. Mod. Phys. A* **19**, 317 (2004).
- [2] E. Leader and E. Predazzi, *An Introduction to Gauge Theories and the New Physics* (Cambridge Univ. Press., Cambridge, 1982).
- [3] G. Gelmini, P. Gondolo, V. Varietieschi, *Phys. Rev.* **D61**, 036005 (2000); R. Ghandi, C. Quigg, M.H. Reno, I. Sarcevic, *Phys. Rev.* **D58**, 093009 (1998).
- [4] C.G. Duan, G.L. Li and P.N. Shen, *Eur. Phys. J. C* (to appear) (2006), arXiv:hep-ph/0604146.
- [5] D. Drakoulakos et al. [Minerva Collaboration], FERMILAB-PROPOSAL-0938; arXiv:hep-ex/0405002.
- [6] S. Kumano, in *AIP Conf. Proc.* 721, pp. 29-36 (2004), arXiv:hep-ph/0310166.
- [7] A. H. Mueller, *Nucl. Phys.* **B335** (1990) 115; N.N. Nikolaev and B.G. Zakharov, *Z. Phys.* **C49** (1991) 607.
- [8] N. Armesto, *Eur. Phys. J. C* **26** (2002) 35.
- [9] J. Forshaw, R. Sandapen and R. Shaw, arXiv:hep-ph/0608161.
- [10] A. Ayala, M.B. Gay Ducati and E. Levin, *Phys. Rev.* **D59**, 054010 (1999).
- [11] A.M. Staśto, K. Golec-Biernat and J. Kwieciński, *Phys. Rev. Lett.* **86** (2001) 596.
- [12] S. Munier, S. Wallon, *Eur. Phys. J. C* **30** (2003) 359.
- [13] A. Freund, K. Rummukainen, H. Weigert and A. Schafer, *Phys. Rev. Lett.* **90**, 222002 (2003).
- [14] V. P. Goncalves and M. V. T. Machado, *Phys. Rev. Lett.* **91**, 202002 (2003).
- [15] C. Marquet and L. Schoeffel, *Phys. Lett.* **B39** (2006) 471.
- [16] V. Barone, M. Genovese, N.N. Nikolaev, E. Predazzi and B.G. Zakharov *Phys.Lett.* **B292** (1992) 181.
- [17] V. Barone, M. Genovese, N.N. Nikolaev, E. Predazzi and B.G. Zakharov *Phys.Lett.* **B328** (1994) 143.
- [18] K. Kutak and J. Kwieciński, *Eur. Phys. J. C* **29**, 521 (2003).
- [19] J. Kwieciński, A.D. Martin, A.M. Staśto, *Phys. Rev.* **D59** (1999) 093002.

- [20] K. Golec-Biernat and M. Wüsthoff, Phys. Rev. **D59** (1999) 014017, *ibid.* **D60** (1999) 114023.
- [21] E. Iancu, K. Itakura and S. Munier, Phys. Lett. B **590**, 199 (2004).
- [22] A.H. Mueller and D.N. Triantafyllopoulos, Nucl. Phys. **B640** (2002) 331; D.N. Triantafyllopoulos, Nucl. Phys. **B648** (2003) 293; A.H. Mueller, Nucl. Phys. **A724** (2003) 223.
- [23] E. Levin and K. Tuchin, Nucl. Phys. **B573** (2000) 833.
- [24] I. Balitsky, Nucl. Phys. **B463** (1996) 99; Yu.V. Kovchegov, Phys. Rev. **D60** (1999) 034008; *ibid.* **D61** (2000) 074018.
- [25] E. Iancu, R. Venugopalan, hep-ph/0303204.
- [26] A. Donnachie and P.V. Landshoff, Phys. Lett. **B518**, 63 (2001).
- [27] C. W. De Jager, H. De Vries, C. De Vries, Atom. Data Nucl. Data Tabl. **14**, 479 (1974).
- [28] N. Armesto, C. A. Salgado and U. A. Wiedemann, Phys. Rev. Lett. **94**, 022002 (2005).
- [29] M.V.T. Machado, Phys. Rev. **D71** (2005) 114009.
- [30] M.V.T. Machado, Phys. Rev. **D70** (2004) 053008.
- [31] W.G. Seligman et al. [CCFR Coll.], Phys. Rev. Lett. **79** (1997) 1213.
- [32] B.T. Fleming et al. [CCFR Coll.], Phys. Rev. Lett. **86** (2001) 5430.
- [33] M. Tzanov et al. [NuTeV Coll.], Phys. Rev. **D74** (2006) 012008.
- [34] R. Fiore and V.R. Zoller, JETP Lett. **82** (2005) 385.
- [35] R. Fiore and V.R. Zoller, Phys. Lett. **B632** (2006) 87.
- [36] U.K. Yang et al., Phys. Rev. Lett. **86** (2001) 2742.
- [37] U.K. Yang et al., Phys. Rev. Lett. **87** (2001) 251802.